Quantum-Classical Auxiliary Field Quantum Monte Carlo with Matchgate Shadows on Trapped Ion Quantum Computer

Luning Zhao
IonQ
Dec 10th, 2025

Quantum computers have the potential to solve difficult chemistry problems

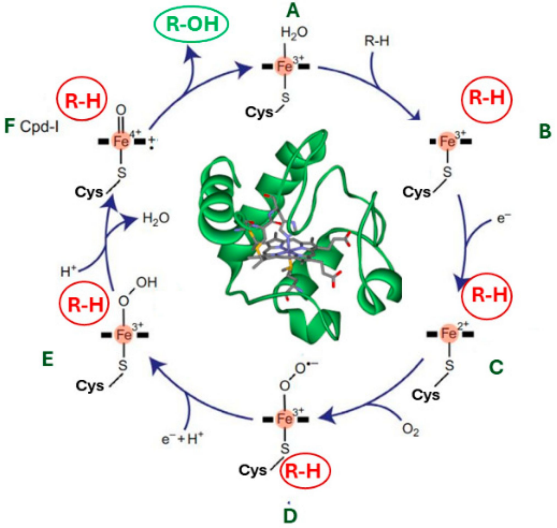

Model complex chemical reactions

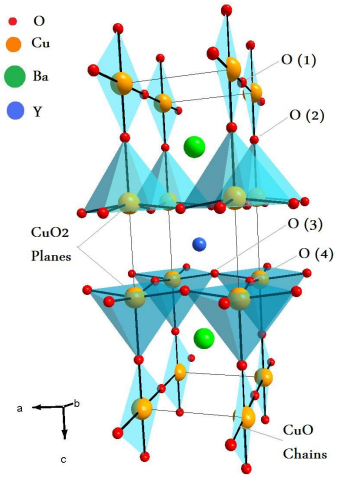

Strongly correlated materials

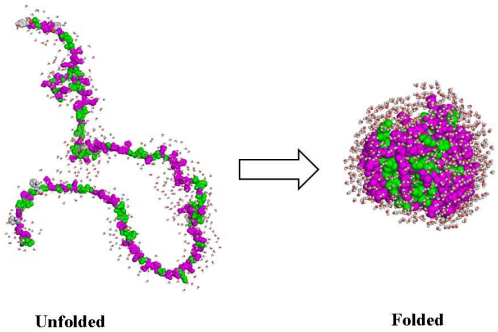

Protein folding

Quantum-Classical Auxiliary-Field Quantum Monte Carlo Carlo

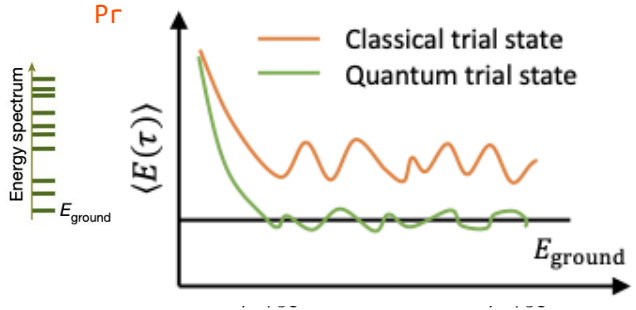

$$|\Psi(\tau)\rangle = \sum_i w_i(\tau)\,|\phi_i(\tau)\rangle$$

Wave function as a linear combination of "walkers"

$$|\phi_i(\tau)\rangle \rightarrow |\phi_i(\tau + \Delta\tau)\rangle$$

$$S_i(\tau) = \frac{\langle \Psi_T | \phi_i(\tau + \Delta\tau)\rangle}{\langle \Psi_T | \phi_i(\tau)\rangle}$$

each walker has a weight defined by the trial wave function

The choice of the trial state is crucial:

- classically only HF could be used efficiently
- HF is not accurate enough
- one could use VQE state as the trial state
- more accurate trial state -> more accurate predictions

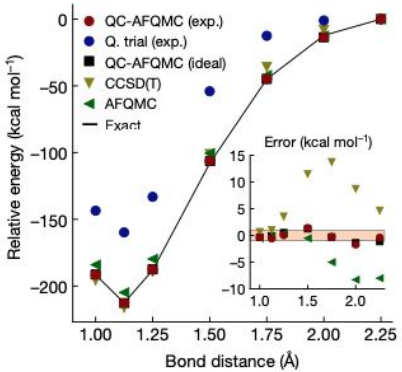

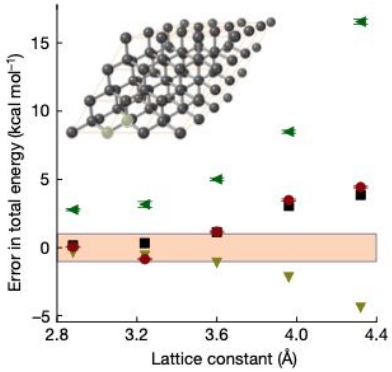

Nature 2021, 603, 416-420

Quantum-Classical Auxiliary-Field Quantum Monte Carlo

Prepare the quantum state

$$\rho = \frac{1}{2}(|0\rangle + |\Psi_T\rangle)(\langle 0| + \langle \Psi_T|)$$

Overlaps become expectation values

$$\langle \Psi_T | \phi_i \rangle = 2\mathrm{tr}(|\phi_i\rangle \langle 0| \rho)$$

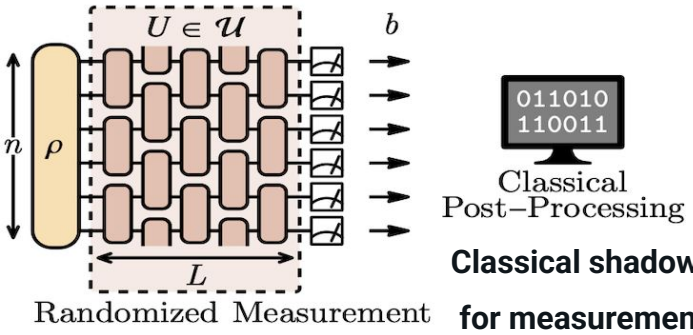

Classical shadows for measurement

Number of Measurement on Quantum Computers

$$\sqrt{N}\log(N)/\varepsilon^2$$

Cost of Classical Post-Processing

Evaluation of Overlaps (need for every time step): $O(N^{4.5})$

Evaluation of Energies (only need at the end of propagation): $O(N^{8.5})$

Nature 2021, 603, 416-420
Commun. Math. Phys. 2023, 629-700

The Post-Processing Bottleneck

Overlap between the trial state and a determinant $\langle \Psi | \phi_p \rangle$

$$\mathbf{B}_{p|b\rangle} = \mathbf{W}^* \mathbf{M}_\phi \mathbf{Q}_p^T \mathbf{C}_{|b\rangle} \mathbf{Q}_p \mathbf{M}_\phi^T \mathbf{W}^\dagger$$

$$\mathbf{A}_{p|b\rangle}(z) = \mathbf{C}_{|\mathbf{0}\rangle}^{(s)} + z \cdot \mathbf{B}_{p|b\rangle}^{(s)}$$

$$\text{Pfaffian of } \mathbf{A}_{p|b\rangle}(z) = \sum_x^l c_{p|b\rangle x} z^x$$

→ Matrix product : $O(N^3) \times O(N^{0.5}) = O(N^{3.5})$
Pfaffian : $O(N^{3.5}) \times O(N) = O(N^{4.5})$

Force bias and local energy

$$\frac{\langle \Psi_T | v_\gamma | \phi \rangle}{\langle \Psi_T | \phi \rangle} = i \frac{\langle \Psi_T | \sum_{pq} L_{pq}^\gamma a_p^\dagger a_q | \phi \rangle}{\langle \Psi_T | \phi \rangle}$$

→ $O(N^3)$ Pfaffians : $O(N^{7.5})$

$$\sum_\gamma \frac{\langle \Psi_T | \sum_{pqrs} L_{pq}^\gamma L_{rs}^\gamma a_p^\dagger a_q a_r^\dagger a_s | \phi \rangle}{\langle \Psi_T | \phi \rangle}$$

→ $O(N^4)$ Pfaffians : $O(N^{8.5})$

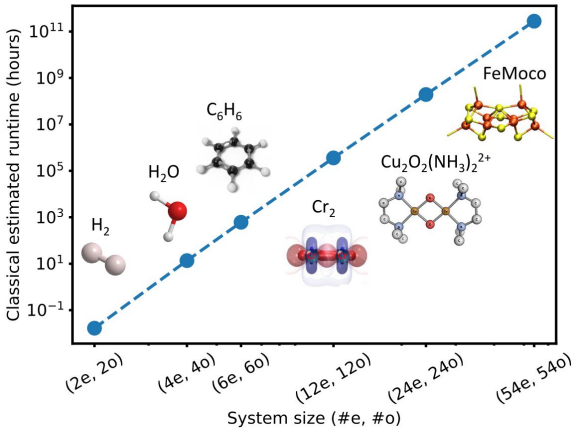

Phys. Rev. Research **6**, 043063, 2024

The Post-Processing Bottleneck

Improvements using finite difference: (Tong *et al*)

Force bias is a first order derivative of overlaps

$$\frac{\langle \Psi_T | v_\gamma | \phi \rangle}{\langle \Psi_T | \phi \rangle} = i \frac{\langle \Psi_T | \sum_{pq} L^\gamma_{pq} a^\dagger_p a_q | \phi \rangle}{\langle \Psi_T | \phi \rangle} = i \frac{\partial}{\partial \lambda} \ln \langle \Psi_T | e^{\lambda \sum_{pq} L^\gamma_{pq} a^\dagger_p a_q} | \phi \rangle \big|_{\lambda=0} = i \frac{\partial}{\partial \lambda} \ln \langle \Psi_T | \tilde{\phi}(\lambda) \rangle \big|_{\lambda=0}$$

Local energy is a second order derivative of overlaps

$$\begin{aligned}
&\sum_\gamma \frac{\langle \Psi_T | \sum_{pqrs} L^\gamma_{pq} L^\gamma_{rs} a^\dagger_p a_q a^\dagger_r a_s | \phi \rangle}{\langle \Psi_T | \phi \rangle} \\
&= \sum_\gamma \frac{\partial^2}{\partial \lambda_1 \partial \lambda_2} \langle \Psi_T | e^{\lambda_1 \sum_{pq} L^\gamma_{pq} a^\dagger_p a_q} e^{\lambda_2 \sum_{rs} L^\gamma_{rs} a^\dagger_r a_s} | \phi \rangle \big|_{\lambda_1=0,\lambda_2=0} / \langle \Psi_T | \phi \rangle \\
&= \sum_\gamma \frac{\partial^2}{\partial \lambda_1 \partial \lambda_2} \langle \Psi_T | \tilde{\phi}(\lambda_1, \lambda_2) \rangle \big|_{\lambda_1=0,\lambda_2=0} / \langle \Psi_T | \phi \rangle ,
\end{aligned}$$

Evaluating with finite difference

Force Bias : $O(N^{5.5})$

Local Energy : $O(N^{5.5})$

Phys. Rev. Research **7**, 012038, 2024

The Post-Processing Bottleneck

Improvements using algorithmic differentiation: (This work)

Force bias

$$\frac{\partial \mathrm{Pf}(\mathbf{A}(\lambda))}{\partial \lambda} = \frac{\mathrm{Pf}(\mathbf{A}(\lambda))}{2} \mathrm{Tr}(\mathbf{A}(\lambda)^{-1} \frac{\partial \mathbf{A}}{\partial \lambda})|_{\lambda=0},$$

Local energy

$$\begin{aligned}
&\frac{\partial^2 \mathrm{Pf}(\mathbf{A}(\lambda_1,\lambda_2))}{\partial\lambda_1\partial\lambda_2} \\
&= \frac{\mathrm{Pf}(\mathbf{A}(\lambda_1,\lambda_2))}{2} \Big\{ \mathrm{tr}\left[\mathbf{A}^{-1}(\lambda_1,\lambda_2)\frac{\partial^2\mathbf{A}(\lambda_1,\lambda_2)}{\partial\lambda_1\partial\lambda_2}\right] \\
&-\mathrm{tr}\left[\mathbf{A}^{-1}(\lambda_1,\lambda_2)\frac{\partial\mathbf{A}(\lambda_1,\lambda_2)}{\partial\lambda_1}\mathbf{A}^{-1}(\lambda_1,\lambda_2)\frac{\partial\mathbf{A}(\lambda_1,\lambda_2)}{\partial\lambda_2}\right] \\
&+\frac{1}{2}\mathrm{tr}\left[\mathbf{A}^{-1}(\lambda_1,\lambda_2)\frac{\partial\mathbf{A}(\lambda_1,\lambda_2)}{\partial\lambda_1}\right]\mathrm{tr}\left[\mathbf{A}^{-1}(\lambda_1,\lambda_2)\frac{\partial\mathbf{A}(\lambda_1,\lambda_2)}{\partial\lambda_2}\right]\Big\}|_{\lambda_1=0,\lambda_2=0}
\end{aligned}$$

Evaluating with algorithmic differentiation

Force Bias : $O(N^{5.5})$->$O(N^{4.5})$

Local Energy : $O(N^{5.5})$->$O(N^{5.5})$

- **No errors due to finite differences**
- **Computational bottleneck transferred from Pfaffians to matrix products**

arXiv:2506.224081v1, 2025

Comparison of Algorithms

Algorithm	Overlap	Force Bias	Local Energy	Bottleneck	GPU?
***Huggins et al* (2022)**	$O(e^N)$	$O(e^N)$	$O(e^N)$	Matrix Product	No
* a theory paper was published later by the Google team to address the exponential scaling, which is used on all later studies, including ours					
Huang et al (2024), first implementation of matchgate post-processing	$O(N^{4.5})$	$O(N^{7.5})$	$O(N^{8.5})$	Matrix Pfaffian	No
Tong et al (2024), numerical differentiation	$O(N^{4.5})$	$O(N^{5.5})$	$O(N^{5.5})$	Matrix Pfaffian	No
Our work (2025), analytical differentiation + GPUs	$O(N^{4.5})$	$O(N^{4.5})$	$O(N^{5.5})$	Matrix Product	Yes

Nature 2021, 603, 416-420
Phys. Rev. Research **6**, 043063, 2024
Phys. Rev. Research **7**, 012038, 2024
arXiv:2506.224081v1, 2025

Quantum-Classical Auxiliary-Field Quantum Monte Carlo

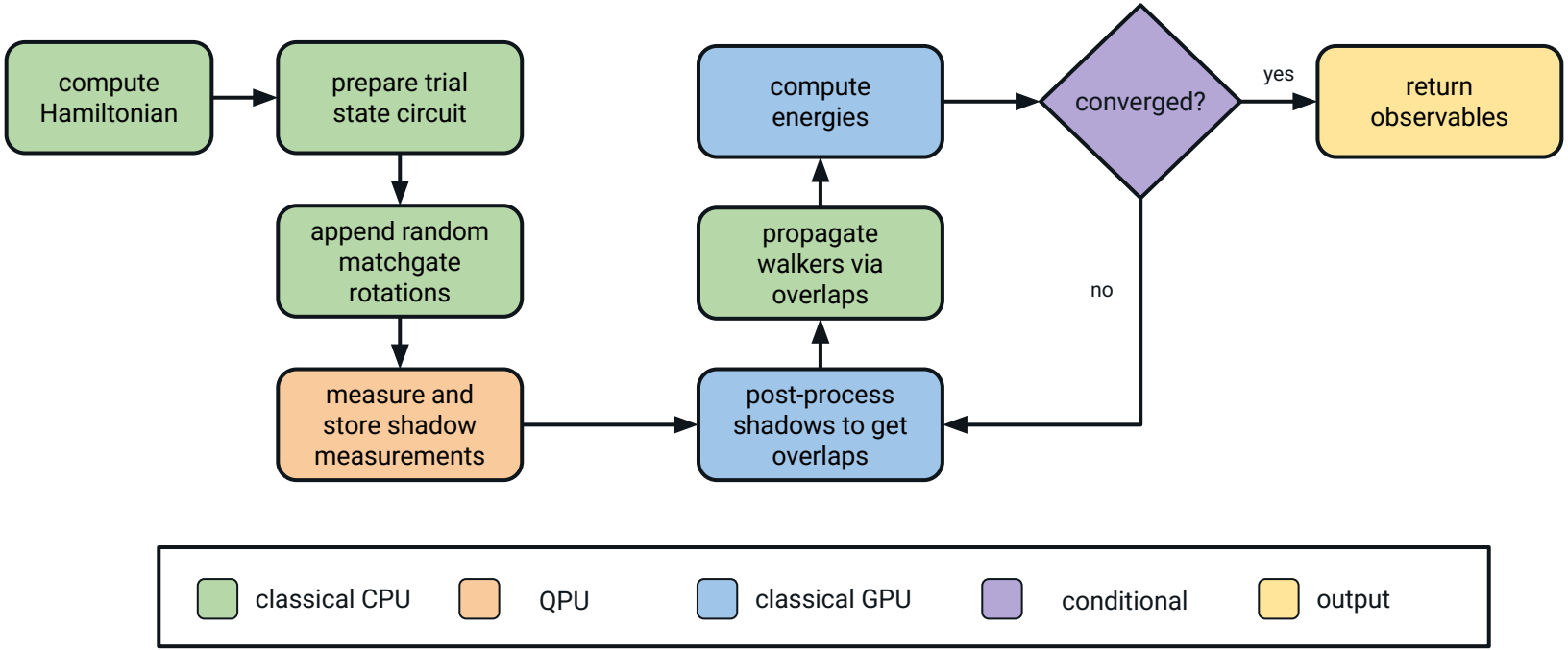

Quantum-Classical Auxiliary-Field Quantum Monte Carlo

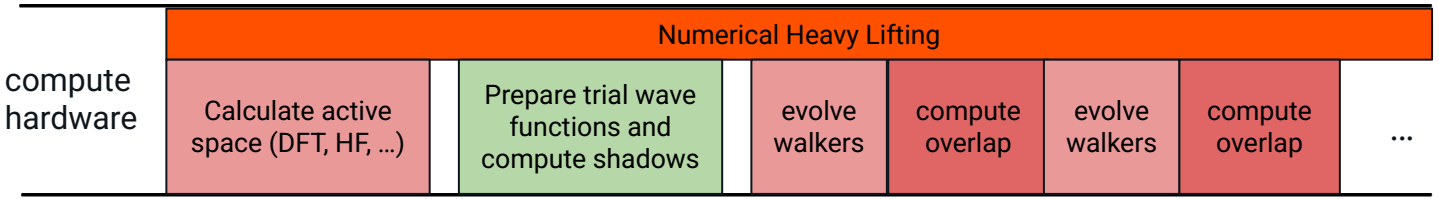

Amazon Braket

IonQ Forte-1

- Trial state preparation
- 24 qubits
- 59,000 shots per molecule

AWS ParallelCluster

Nvidia H200 Tensor Core GPU

- Post processing for 3 molecules
- 40 P5en instances (8 GPUs per instance)

The Virtual Correlation Energy

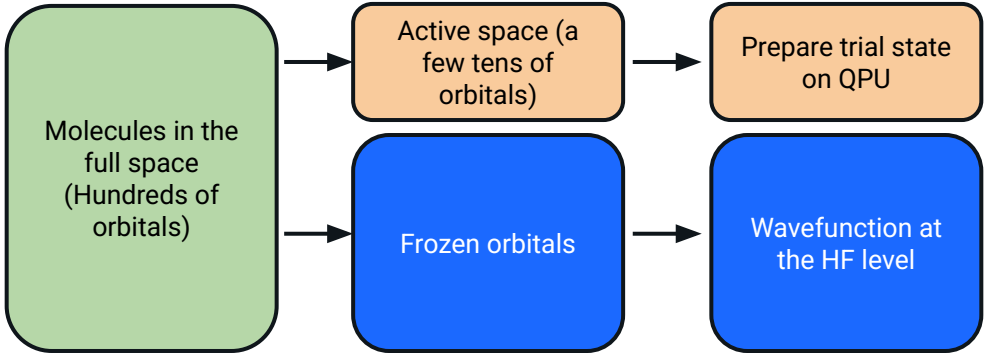

Overall Trial State

$$|\Psi_T\rangle = |\Xi_c\rangle \otimes |\Psi_{T,a}\rangle \otimes |0_v\rangle$$

Overlaps

$$\langle \Psi_T | \phi \rangle = \det(\Sigma_c R) \langle \Psi_{T,a} | \tilde{\phi}_a \rangle \det(U^\dagger)\det(V)$$

Measure on QPU

Compute classically

- **Allows one to incorporate dynamic correlation outside of the active space**
- **Minimum computational overhead**

arXiv:2506.224081v1, 2025

The Suzuki-Miyaura Reaction

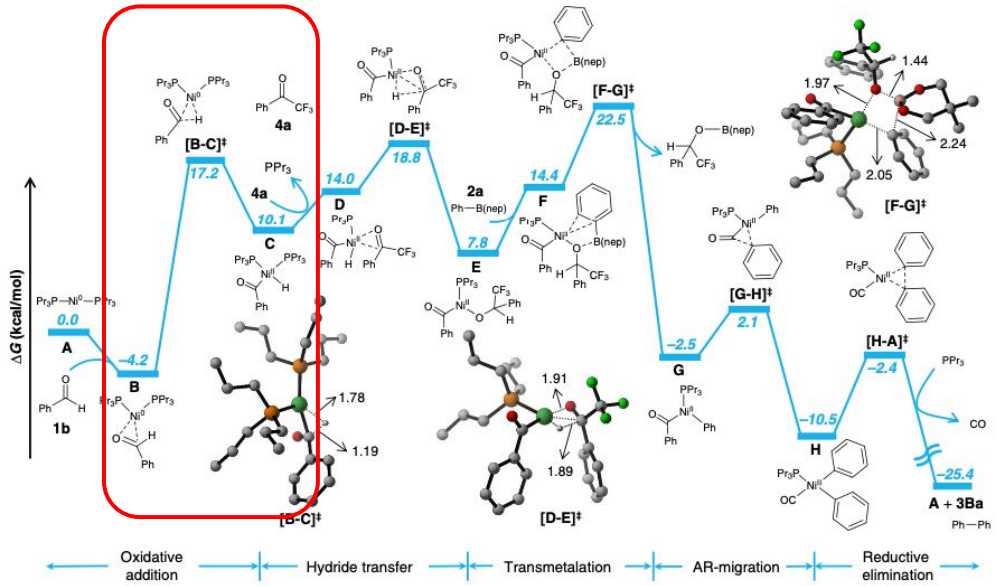

Ni-catalyzed deformylative Suzuki–Miyaura cross coupling

130 orbitals in total , 16 qubits in active space

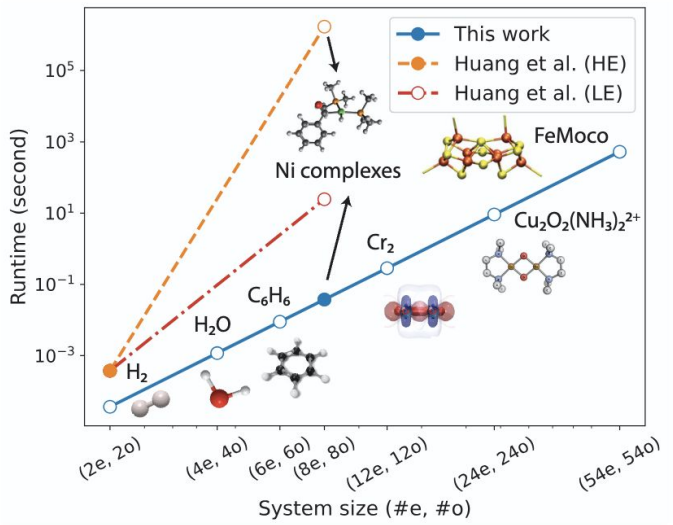

<1 hr
Laptop

32 nrs
Forte

00

Nat. Commun. 10:1957, 2019.
arXiv:2506.224081v1, 2025

Results on QPU and Simulators

Percentage of Correlation Energy Captured

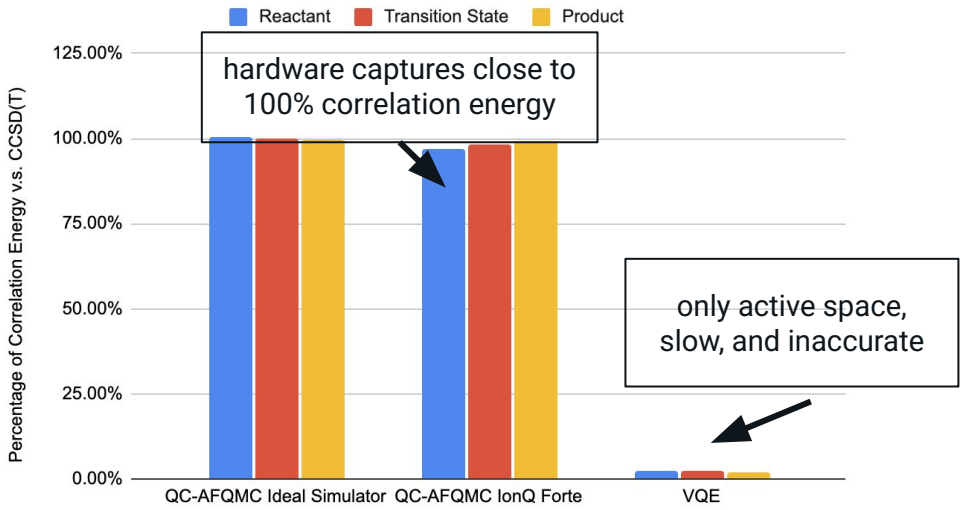

Reaction barrier

Method	B → [B-C]‡	C → [B-C]‡
DFT[a]	21.4	7.1
RHF	77.4	85.3
CCSD(T)	53.3	45.4
VQE/upCCD	75.1	80.5
ph-AFQMC[b]	62(4)	76(5)
QC-AFQMC (Ideal simulator)	57(4)	44(4)
QC-AFQMC (Forte QPU)	43(3)	55(3)

[a] Free energies in solution [SMD (1,4-Dioxane)] evaluated with M06/Def2-TZVPP//ωB97xD/Def2-TZVP(Ni)/Def2-SVP(non-metal).[47]

[b] Using a single RHF Slater determinant as a trial state.

arXiv:2506.224081v1, 2025

Results on QPU and Simulators

Percentage of Correlation Energy Captured

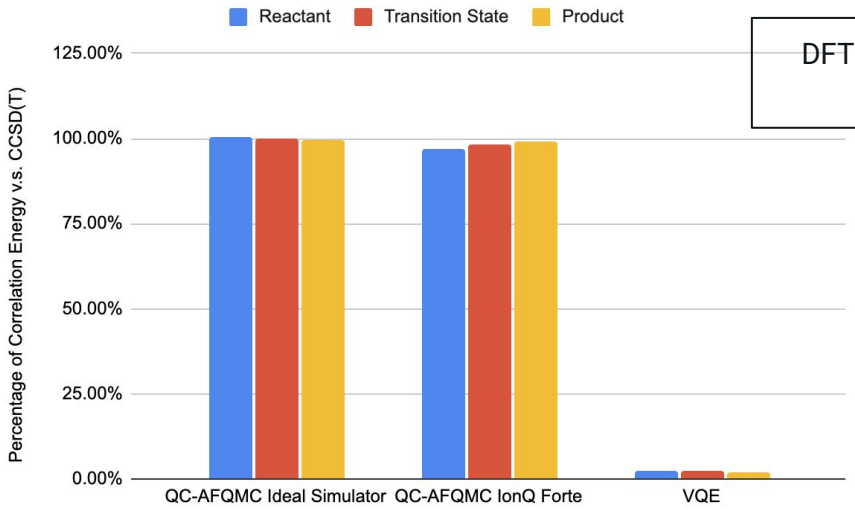

DFT underestimate the barrier

Reaction barrier

Method	B → [B-C]‡	C → [B-C]‡
DFT[a]	21.4	7.1
RHF	77.4	85.3
CCSD(T)	53.3	45.4
VQE/upCCD	75.1	80.5
ph-AFQMC[b]	62(4)	76(5)
QC-AFQMC (Ideal simulator)	57(4)	44(4)
QC-AFQMC (Forte QPU)	43(3)	55(3)

[a] Free energies in solution [SMD (1,4-Dioxane)] evaluated with M06/Def2-TZVPP//ωB97xD/Def2-TZVP(Ni)/Def2-SVP(non-metal).[47]

[b] Using a single RHF Slater determinant as a trial state.

arXiv:2506.224081v1, 2025

Results on QPU and Simulators

Percentage of Correlation Energy Captured

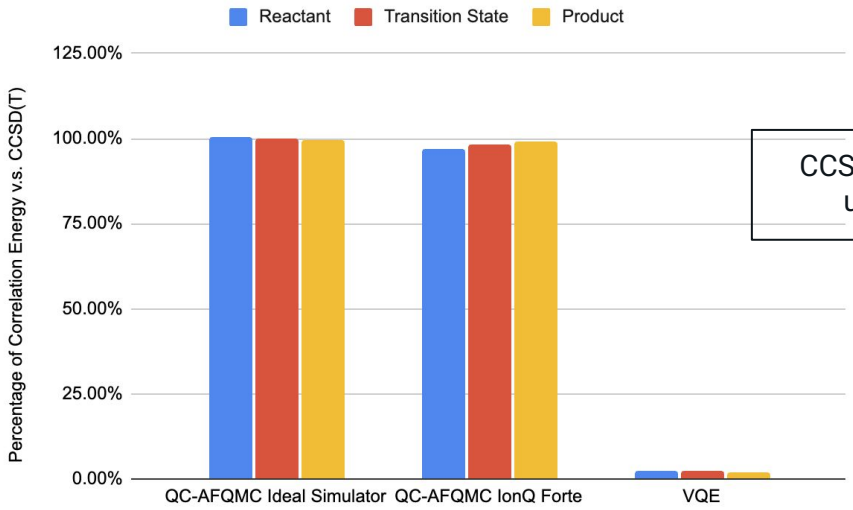

CCSD(T) gets rid of the underestimation

Reaction barrier

Method	B → [B-C]‡	C → [B-C]‡
DFT[a]	21.4	7.1
RHF	77.4	85.3
CCSD(T)	53.3	45.4
VQE/upCCD	75.1	80.5
ph-AFQMC[b]	62(4)	76(5)
QC-AFQMC (Ideal simulator)	57(4)	44(4)
QC-AFQMC (Forte QPU)	43(3)	55(3)

[a] Free energies in solution [SMD (1,4-Dioxane)] evaluated with M06/Def2-TZVPP//ωB97xD/Def2-TZVP(Ni)/Def2-SVP(non-metal).[47]

[b] Using a single RHF Slater determinant as a trial state.

arXiv:2506.224081v1, 2025

Results on QPU and Simulators

Percentage of Correlation Energy Captured

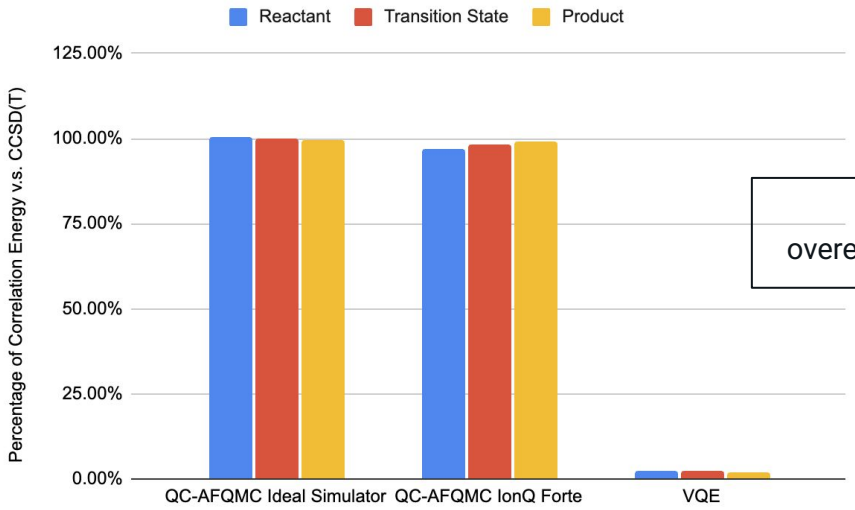

RHF and VQE overestimates the barrier

Reaction barrier

Method	B → [B-C]‡	C → [B-C]‡
DFT[a]	21.4	7.1
RHF	77.4	85.3
CCSD(T)	53.3	45.4
VQE/upCCD	75.1	80.5
ph-AFQMC[b]	62(4)	76(5)
QC-AFQMC (Ideal simulator)	57(4)	44(4)
QC-AFQMC (Forte QPU)	43(3)	55(3)

[a] Free energies in solution [SMD (1,4-Dioxane)] evaluated with M06/Def2-TZVPP//ωB97xD/Def2-TZVP(Ni)/Def2-SVP(non-metal).[47]

[b] Using a single RHF Slater determinant as a trial state.

arXiv:2506.224081v1, 2025

Results on QPU and Simulators

Percentage of Correlation Energy Captured

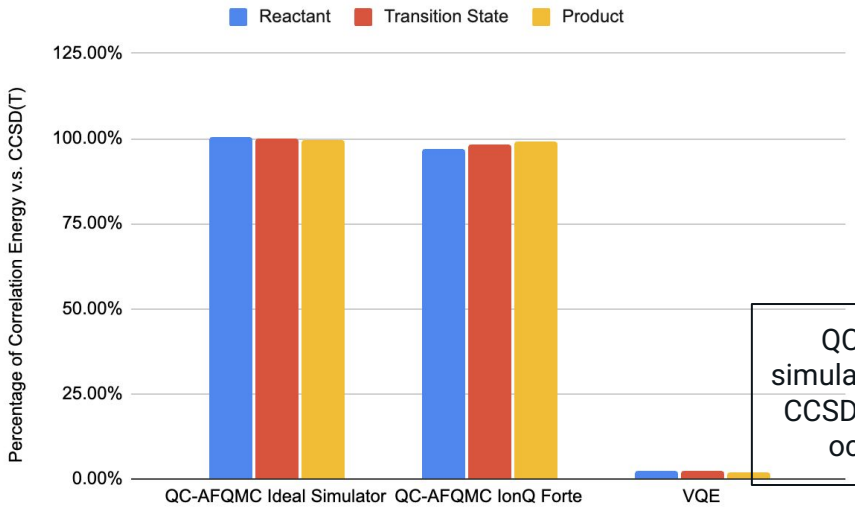

QC-AFQMC on ideal simulator closes agree with CCSD(T), but some errors occur on hardware

Reaction barrier

Method	B → [B-C]‡	C → [B-C]‡
DFT[a]	21.4	7.1
RHF	77.4	85.3
CCSD(T)	53.3	45.4
VQE/upCCD	75.1	80.5
ph-AFQMC[b]	62(4)	76(5)
QC-AFQMC (Ideal simulator)	57(4)	44(4)
QC-AFQMC (Forte QPU)	43(3)	55(3)

[a] Free energies in solution [SMD (1,4-Dioxane)] evaluated with M06/Def2-TZVPP//ωB97xD/Def2-TZVP(Ni)/Def2-SVP(non-metal).[47]

[b] Using a single RHF Slater determinant as a trial state.

arXiv:2506.224081v1, 2025

Conclusions

What are the advantages of QC-AFQMC and future research directions?

Efficient quantum and classical processing

Improved algorithmic improvements in this work made the method more practical and becomes comparable to classical counterparts

Noise resilient and efficient

Compared with VQE, QC-AFQMC is much more noise resilient and efficient (no feedback loops between the QPU and CPU)

Error Mitigation needed

To deliver chemical accuracy, one still needs to apply error mitigation techniques

Leverage QPU + CPU + GPU

QC-AFQMC is a perfect method for QPU + CPU + GPU hybrid computing

Can treat large systems

with the aid of virtual correlation energy, QC-AFQMC is able to capture correlations inside and outside the active space

Acknowledgements


Joshua J. Goings


Arseny Kovyrshin


Jeff Hammond

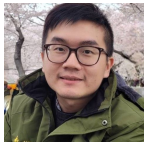
Tim Chen


Michael Brett


Evgeny Epifanovsky


Lars Tornberg


Zohim Chandani


Benchen Huang


Tyler Y. Takeshita


Martin Roetteler


Anders Broo

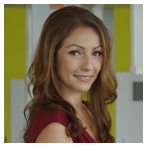
Elica Kyoseva


Eric Kessler

and many others!